

Real-Time Monitoring of Oxidative Burst from Single Plant Protoplasts Using Microelectrochemical Sensors Modified by Platinum Nanoparticles

Feng Ai,[†] Hong Chen,[‡] Shu-Hui Zhang,[†] Sheng-Yi Liu,[‡] Fang Wei,[‡] Xu-Yan Dong,[‡] Jie-Ke Cheng,[†] and Wei-Hua Huang^{*†}

Key Laboratory of Analytical Chemistry for Biology and Medicine (Ministry of Education), College of Chemistry and Molecular Sciences, Wuhan University, Wuhan 430072, China, and Key Laboratory of Oil Crops Biology of the Ministry of Agriculture, Oil Crops Research Institute, Chinese Academy of Agricultural Sciences, Wuhan, 430062, China

Oxidative bursts from plants play significant roles in plant disease defense and signal transduction; however, it has not hitherto been investigated on individual living plant cells. In this article, we fabricated a novel sensitive electrochemical sensor based on electrochemical deposition of Pt nanoparticles on the surface of carbon fiber microdisk electrodes via a nanopores containing polymer matrix, Nafion. The numerous hydrophilic nanochannels in the Nafion clusters coated on the electrode surface served as the molecular template for the deposition and dispersion of Pt, which resulted in the uniform construction of small Pt nanoparticles. The novel sensor displayed a high sensitivity for detection of H₂O₂ with a detection limit of 5.0×10^{-9} M. With the use of this microelectrochemical sensor, the oxidative burst from individual living plant protoplasts have been real-time monitored for the first time. The results showed that oxidative burst from single protoplasts triggered by a pathogen analogue were characterized by quanta release with a large number of “transient oxidative microburst” events, and protoplasts from the transgenic plants biologically displayed better disease-resistance and showed a distinguished elevation and longer-lasting oxidative burst.

Reactive oxygen species (ROS) are generally small highly reactive molecules containing oxygen, which have been proved to be signaling molecules that control cell proliferation and cell death to regulate plant growth and development, adaptation to abiotic stress factors, and proper responses to pathogen attack.^{1–3} Experimental results showed that inoculation of plant tissues with pathogens or treatments of cell cultures with microbial elicitors causes an oxidative burst characterized by the rapid generation

of hydrogen peroxide.^{4,5} However the ROS mechanisms are mostly hypothesized or based upon the local and systemic observation in tissues, leaves, or cell populations. Deeper understanding of the ROS mechanism in plant disease defense and signal transduction necessitates the real-time kinetic and quantitative monitoring of the oxidative burst at the single-cell level. However, such investigations have not hitherto been reported on individual living plant cells.

The electrochemical technique based on ultramicroelectrodes, owing to its unique characteristics of high sensitivity, fast response, and small geometric size, plays a significant role in real-time monitoring of chemical messengers released from single secretory cells and demonstrates the mechanisms of vesicular exocytosis.^{6–11} This technique has also been successfully used in the investigation of oxidative stress from single mammalian cells or tissues.^{12–16}

Platinized carbon fiber microelectrodes (CFMEs) are of great interest to real-time monitor ROS at single cells, thanks to the high tenacity and high elasticity modulus of the carbon fiber and the excellent electrochemical catalysis of Pt to ROS.^{9,12–14,17} It is

- (4) Wu, G.; Shortt, B. J.; Lawrence, E. B.; Levine, E. B.; Fitzsimmons, K. C.; Shah, D. M. *Plant Cell* **1995**, *7*, 1357–1368.
- (5) Orozco-Cárdenas, M. L.; Narváez-Vásquez, J.; Ryan, C. A. *Plant Cell* **2001**, *13*, 179–191.
- (6) Wightman, R. M.; Jankowski, J. A.; Kennedy, R. T.; Kawagoe, K. T.; Schroeder, T. J.; Leszczyszyn, D. J.; Near, J. A.; Diliberto, E. J.; Viveros, O. H. *Proc. Natl. Acad. Sci. U.S.A.* **1991**, *88*, 10754–10758.
- (7) Dernick, G.; Gong, L. W.; Tabares, L.; De Toledo, G. A.; Lindau, M. *Nat. Methods* **2005**, *2*, 699–708.
- (8) Wightman, R. M. *Science* **2006**, *311*, 1570–1574.
- (9) Schulte, A.; Schuhmann, W. *Angew. Chem., Int. Ed.* **2007**, *46*, 8760–8777.
- (10) Amatore, C.; Arbault, S.; Guille, M.; Lemaître, F. *Chem. Rev.* **2008**, *108*, 2585–2621.
- (11) Wang, W.; Zhang, S. H.; Wang, Z. L.; Cheng, J. K.; Huang, W. H. *Anal. Bioanal. Chem.* **2009**, *394*, 17–32.
- (12) Amatore, C.; Arbault, S.; Bruce, D.; Oliveira, P. d.; Erard, M.; Vuillaume, M. *Faraday Discuss.* **2000**, *116*, 319–333.
- (13) Amatore, C.; Arbault, S.; Bouton, C.; Coffi, K.; Drapier, J. C.; Ghandour, H.; Tong, Y. H. *ChemBioChem* **2006**, *7*, 653–661.
- (14) Amatore, C.; Arbault, S.; Bouton, C.; Drapier, J.; Ghandour, H.; Koh, A. C. W. *ChemBioChem* **2008**, *9*, 1472–1480.
- (15) Isik, S.; Schuhmann, W. *Angew. Chem., Int. Ed.* **2006**, *45*, 7451–7454.
- (16) Wang, W.; Xiong, Y.; Du, F. Y.; Huang, W. H.; Wu, W. Z.; Wang, Z. L.; Cheng, J. K.; Yang, Y. F. *Analyst* **2007**, *132*, 515–518.
- (17) Arbault, S.; Pantano, P.; Jankowski, J. A.; Vuillaume, M.; Amatore, C. *Anal. Chem.* **1995**, *67*, 3382–3390.

* To whom correspondence should be addressed. E-mail: whhuang@whu.edu.cn. Phone: (86)2787218954. Fax: (86)2768754067.

[†] Wuhan University.

[‡] Chinese Academy of Agricultural Sciences.

(1) Tenhaken, R.; Levine, A.; Brisson, L. F.; Dixon, R. A.; Lamb, C. *Proc. Natl. Acad. Sci. U.S.A.* **1995**, *92*, 4158–4163.

(2) Mittler, R. *Trends Plant Sci.* **2002**, *7*, 405–410.

(3) Gechev, T. S.; Van Breusegem, F.; Stone, J. M.; Denev, I.; Laloi, C. *BioEssays* **2006**, *28*, 1091–1101.

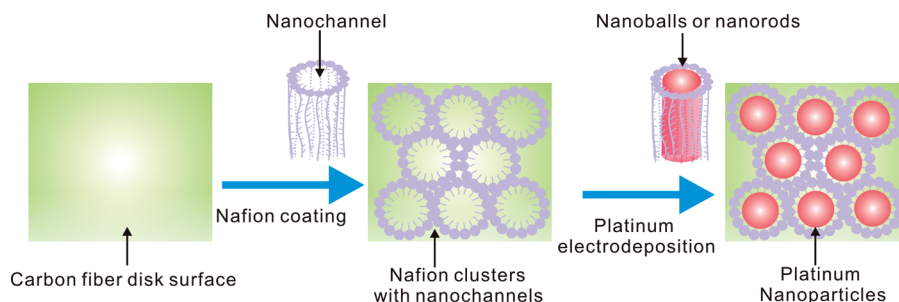


Figure 1. Cartoons showing the principle of the fabrication of Pt nanoparticles modified carbon fiber microdisk electrode (NPs/CFMDE) using Nafion as the template.

essential to enlarge the effective surface area by diminishing the size of Pt particles and distributing them homogeneously on the surface to reduce electrochemical noise and improve detection sensitivity. However, direct electrodeposition of Pt on the electrode surface can hardly prevent the aggregation of Pt particles, which results in deficient detection capabilities. Various methods including direct modification with chemically synthesized nanoparticles^{18,19} or electrodeposition using nanometer-sized frameworks (such as molecular template,²⁰ nanofibers,²¹ and nanotubes²²) have been developed to disperse nanoparticles on the electrode substrate with the diameter ranging from several tens of micrometers to several millimeters. However, few papers have reported on construction of Pt nanoparticles on CFMEs with a diameter of several micrometers.

Polymer matrixes with natural nanopores have been successfully used to synthesize and disperse nanoparticles in the field, for example, catalyst and fuel cell research.^{23–28} Among the polymer matrixes, Nafion is an excellent and widely used proton-exchange polymer composed of numerous hydrophilic ionic pores,^{26,29} and has been used as the framework for the fabrication of nanoparticles such as Ag₂S,³⁰ TiO₂,³¹ and Pt.³² In this article, we used Nafion as the template to electrodeposit Pt nanoparticles on the surface of a carbon fiber microdisk electrode. The electrodeposition of Pt confined to the numerous nanopores or nanochannels inside the Nafion membrane leads to the Pt particles have a well-defined and homogeneous nanostructures

and high specific surface area (Figure 1). This electrochemical sensor showed high sensitivity for detection H₂O₂ with a detection limit of 5.0×10^{-9} M. Using the novel electrochemical sensor, we amperometrically monitored in real-time the oxidative burst from individual living plant protoplasts for the first time, and the results demonstrated that the oxidative burst from single protoplasts triggered by the pathogen analogue benzothiadiazole (BTH) was characterized by quanta release with a large number of “transient oxidative microburst” events.

EXPERIMENTAL SECTION

Fabrication of the Pt Nanoparticles Modified CFMEs.

A carbon fiber microcylindrical electrode (CFMCE) was first made as previously described by our lab,^{33–36} which was then insulated with a nonconducting electrophoresis paint (Kolear Chemical Engineering Corporation, Wuhan, China) layer by electrodeposition with a platinum electrode as the reference electrode. Linear scanning voltammetry (LSV) from -0.5 to -3.0 V at a rate of 0.01 V/s and constant voltage at -3.0 V for 60 s were adopted for first insulation, which was followed by polymerization in an oven at 160 °C for 30 min. Then a second constant voltammetric run was performed at -3.5 V for 60 s and polymerization at 160 °C for 30 min to prevent the problems such as pinholes and congregation. Insulated CFMEs were then cut by a thin and clean blade to form CFMDEs with 100 – 200 μm in shaft length and 5 – 7 μm in diameter under a stereomicroscope.

The CFMDEs were electrochemically activated by continuous cycling of the electrode potential between -0.2 and $+1.800$ V (vs Ag/AgCl) at scan rate of 100 mV/s for 400 s in PBS solution³⁷ before Nafion coating. After being dip-coated in 1% Nafion (different concentrations have been tested, and the electrodes obtained using 1% Nafion displayed the best performance), the electrodes were stereolized in 70 °C for 3 min. The surface of the microelectrode was platinized at a constant potential of -0.07 V in a $\text{Pt}(\text{NH}_3)_6^{4+}$ solution (PtCl_6^{2-} was converted to $\text{Pt}(\text{NH}_3)_6^{4+}$ by adding $\text{NH}_3 \cdot \text{H}_2\text{O}$ to improve electrodeposition performance) where a platinum electrode was used as counter electrode and an Ag/AgCl electrode as the reference electrode. The electro-

- (18) Hrapovic, S.; Liu, Y.; Male, K. B.; Luong, J. H. T. *Anal. Chem.* **2004**, *76*, 1083–1088.
- (19) Guascito, M. R.; Filippo, E.; Malatesta, C.; Manno, D.; Serra, A.; Turco, A. *Biosens. Bioelectron.* **2008**, *24*, 1057–1063.
- (20) Evans, S. A. G.; Elliott, J. M.; Andrews, L. M.; Bartlett, P. N.; Doyle, P. J.; Denuault, G. *Anal. Chem.* **2002**, *74*, 1322–1326.
- (21) Tang, H.; Chen, J.; Nie, L.; Liu, D.; Deng, W.; Kuang, Y.; Yao, S. *J. Colloid Interface Sci.* **2004**, *269*, 26–31.
- (22) Tsai, Y. C.; Hong, Y. H. *J. Solid State Electrochem.* **2008**, *12*, 1293–1299.
- (23) Attard, G. S.; Bartlett, P. N.; Coleman, N. R. B.; Elliott, J. M.; Owen, J. R.; Wang, J. H. *Science* **1997**, *278*, 838–840.
- (24) Lang, H.; May, R. A.; Iversen, B. L.; Chandler, B. D. *J. Am. Chem. Soc.* **2003**, *125*, 14832–14836.
- (25) Alvarez-Puebla, R. A.; Nazri, G.-Abbas; Aroca, R. F. *J. Mater. Chem.* **2006**, *16*, 2921–2924.
- (26) Schmidt-Rour, K.; Chen, Q. *Nat. Mater.* **2007**, *6*, 75–83.
- (27) Ledesma-García, J.; García, I. L. E.; Rodríguez, F. J.; Chapman, T. W.; Godínez, L. A. *J. Appl. Electrochem.* **2008**, *38*, 515–522.
- (28) Jiang, C.; Lin, X. *J. Appl. Electrochem.* **2008**, *38*, 1659–1664.
- (29) Mauritz, K. A.; Moore, R. B. *Chem. Rev.* **2004**, *104*, 4535–4585.
- (30) Rollins, H. W.; Lin, F.; Johnson, J.; Ma, J. J.; Liu, J. T.; Tu, M. H.; DesMarteau, D. D.; Sun, Y. P. *Langmuir* **2000**, *16*, 8031–8036.
- (31) Pathak, P.; Mezziani, M. J.; Li, Y.; Cureton, L. T.; Sun, Y. P. *Chem. Commun.* **2004**, 1234–1235.
- (32) Chou, J.; Jayaraman, S.; Ranasinghe, A. D.; McFarland, E. W.; Buratto, S. K.; Metiu, H. *J. Phys. Chem. B* **2006**, *110*, 7119–7121.

- (33) Huang, W. H.; Pang, D. W.; Tong, H.; Wang, Z. L.; Cheng, J. K. *Anal. Chem.* **2001**, *73*, 1048–1052.
- (34) Huang, W. H.; Cheng, W.; Pang, D. W.; Wang, Z. L.; Cheng, J. K.; Cui, D. F. *Anal. Chem.* **2004**, *76*, 483–488.
- (35) Wu, W. Z.; Huang, W. H.; Wang, W.; Wang, Z. L.; Cheng, J. K.; Xu, T.; Zhang, R. Y.; Chen, Y.; Liu, J. J. *Am. Chem. Soc.* **2005**, *127*, 8914–8915.
- (36) Du, F. Y.; Huang, W. H.; Shi, Y. X.; Wang, Z. L.; Cheng, J. K. *Biosens. Bioelectron.* **2008**, *24*, 415–421.
- (37) Strein, T. G.; Ximba, B. J.; Hamad, A. H. *Electroanalysis* **1999**, *11*, 37–46.

chemical and scanning electron microscope characterization were performed on an electrochemical workstation (CHI 660A, CH Instruments, Shanghai, China) and a scanning electron microscope (Quanta 200, Fei, Holland), respectively.

Protoplasts Separation and Culture. The process and methods for production of the plants have been previously described in detail.³⁸ Susceptible oilseed rape 215 is a self-ed line (>10 generations) and served as explants of genetic transformation. GB 014 is a stably heritable line (the eighth generation) of oilseed rape containing a cDNA encoding glucose oxidase (GO) which was cloned from *Aspergillus niger*. Briefly, the cDNA was inserted into the *Hind III* site of a vector pBI121 to form a plant expression construct pBGO, and then the pBGO was transformed into oilseed rape plant by an *Agrobacterium*-mediated method.

Protoplasts were isolated from a small piece of sterilized oilseed rape leaf about several days old and was chopped into smaller pieces and pre-separated in CPW9M solution (27.2 mg of KH_2PO_4 , 101.0 mg of KNO_3 , 1480.0 mg of $\text{CaCl}_2 \cdot 2\text{H}_2\text{O}$, 246.0 mg of MgSO_4 , 0.16 mg of KI, 0.025 mg of CuSO_4 dissolved in 1 L of superpurified water containing 9% mannitol, pH 5.6) for 30 min. The solution was then replaced by an enzymatic mixture containing 1.0% cellulose, 0.5% pectinase, and 0.05% bovine serum albumin (BSA). The suspension was incubated in darkness for 14 h at 25 °C on the shaking bed at a speed of 30–40 rpm. Then, the suspension was filtered by 45 μm nylon sieve, and the filtrate was centrifuged in 600 rpm for 10 min. The pellet was resuspended in 5 mL of CPW9M and centrifuged twice. Protoplasts were separated from debris by density gradient centrifugation which took 21% and 11% sucrose solution as the flotation medium. The protoplasts in the middle and close to the bottom layer were collected for the next experiments. The isolated protoplasts (15.6 ± 2.3 and 15.9 ± 2.6 μm in average diameter from 215 and GB014 oilseed rapes, respectively) were then put into a Petri dish which was precoated by 0.15% gelatin on the bottom for more than 3 h for adherence and then incubated in phosphate buffered saline (PBS, pH 7.2) for oxidative burst detection. The fluorescein diacetate (FDA) dyeing test was used to analyze the activity of acquired protoplasts.

Real-Time Electrochemical Monitoring of Oxidative Burst from Single Protoplasts and Data Analysis. All the electrochemical monitoring experiments on single protoplasts were performed at room temperature on the stage of an inverted fluorescent microscope (Axiovert 200M, Zeiss, Germany) placed in a faraday cage. A chamber served as an electrolytic cell and was placed on the microscope stage, whose bottom plane was coated with 0.15% gelatin to enhance the adherence of protoplasts. In each oxidative burst measurement, a new Petri dish with cells adhered on it was first washed by PBS twice to remove the remaining medium before being put into the chamber for measuring, then 1 mL of sterilized PBS was added into it. Under the microscope, the microelectrode was first positioned about 50 μm from the isolated protoplast of interest and polarized for 5 min, and then the sensor's tip was precisely positioned to slightly touch the cell surface for amperometric monitoring by a micromanipulator (TransferMan NK2, Eppendorf, Hamburg, Germany).

On the opposite side, a glass microcapillary filled with 10 μL of 0.1 mM BTH connected to a manual piston pump (CellTram Oil, Eppendorf, Hamburg, Germany) was positioned by another micromanipulator (TransferMan NK2, Eppendorf, Hamburg, Germany) to the place where the distance between the cell and the outlet of the microcapillary was about 50 μm to induce the oxidative burst. The oxidative burst from single protoplasts was amperometrically recorded by a patch clamp amplifier (EPC10, Heka Elektronik, Germany) at a constant potential of 600 mV. Signals were sampled at 20 kHz, bessel filtered at 2.9 kHz, and digitally filtered at 1 kHz, and raw amperometric data were collected using "Pulse" and then analyzed by Igor Pro (Igor Pro, Wave Metrics) and Minianalysis 6.0 software. Only events larger than 5-fold the root-mean-square (rms) noise were taken as oxidative microburst events and used for analysis.

RESULTS AND DISCUSSION

Fabrication and Characterization of NPts/CFME. Here we used Nafion, an excellent perfluorinated cation-exchange membrane composed of numerous hydrophilic ionic pores with diameters on the order of several nanometers,^{26,29} as the molecular template to electrochemically deposit Pt nanoparticles on the surface of CFMDE. Our results showed that direct electrodeposition using PtCl_6^{2-} on Nafion coated CFMDE resulted in poor electrodeposition efficiency and unfavorable detection performance on H_2O_2 , possibly owing to the repulsion force between PtCl_6^{2-} and SO_3^- groups on the Nafion structure. In order to prevent the repulsive force, PtCl_6^{2-} was converted to $\text{Pt}(\text{NH}_3)_6^{4+}$ by adding $\text{NH}_3 \cdot \text{H}_2\text{O}$ and the $\text{Pt}(\text{NH}_3)_6^{4+}$ cations could be ion-exchanged into Nafion films.³⁹ The absorption of $\text{Pt}(\text{NH}_3)_6^{4+}$ on the Nafion surface not only dramatically improve the Pt electrodeposition efficiency but also benefit the uniform dispersion of Pt nanoparticles. In addition, the catalytic capabilities of microsensors platinized with a series of electric quantities such as 20, 15, 8, 4, and 2 μC have been investigated, respectively, and results showed that using 2–4 μC lead to the best detection capability of H_2O_2 for a CFMDE with the diameter of 7 μm .

Figure 2 showed the scanning electron microscope (SEM) pictures of the microelectrochemical sensors, comparing the electrodes obtained from direct electrodeposition of Pt on CFMDE (Figure 2A) where the Pt granules were intensively aggregated owing to the agglomeration in electrodeposition. However, electrodeposition on Nafion precoated CFMDEs resulted in numerous homogeneously distributed Pt nanoparticles on the surface of CFMDEs (Figure 2B–D). The results indicated that the polymer matrix, Nafion, compelled the deposition of Pt to be confined inside the numerous hydrophilic nanopores or nanochannels inside the Nafion membrane, and the agglomeration of unstable Pt nanoparticles was successfully prevented. The well-defined and homogeneous platinum nanostructures on the electrode surface provided high specific surface area to improve the detection sensitivity of ROS.

The results from amperometric detection of H_2O_2 demonstrated that, comparing with the electrodes obtaining from direct electrodeposition of Pt on CFMDEs (Pt/CFMDE, Figure

(38) Dong, X. B.; Ji, R. Q.; Guo, X. L.; Foster, S. J.; Chen, H.; Dong, C. H.; Liu, Y. Y.; Hu, Q.; Liu, S. Y. *Planta* **2008**, 228, 331–340.

(39) Thompson, S. D.; Jordan, L. R.; Forsyth, M. *Electrochim. Acta* **2001**, 46, 1657–1663.

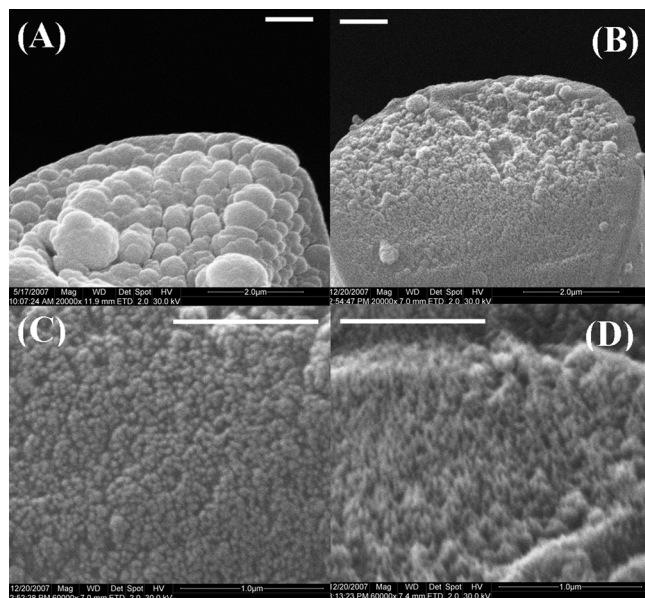


Figure 2. SEM images of (A) the surface of a platinum modified carbon fiber microdisk electrode (Pt/CFMDE) and (B–D) the surface of the Pt nanoparticles modified on Nafion precoated CFMDE (NPTs/CFMDE); the scale bars represent 1 μm .

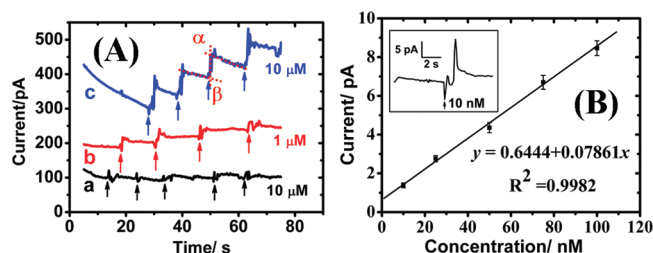


Figure 3. (A) Amperometric response curves of a Pt/CFMDE (a) and a NPTs/CFMDE (b,c) to a series of increases of H_2O_2 concentration in a stirred deaerated PBS solution (pH 7.4). The amperometric response was defined as the current between “ α ” (intersection point of the extension line of the averaged upper baseline and the vertical line at the time H_2O_2 is added) and “ β ” (the intersection point of the extension line of the averaged lower baseline and the vertical line at the time H_2O_2 is added). (B) The calibration curve for H_2O_2 solution over the concentration range from 10 to 100 nM, and the amperometric response to 10 nM H_2O_2 is magnified in the inset.

3A, curve a) and CFMDE (data not shown), the NPTs/CFMDE show a dramatically improved sensitivity (Figure 3A, curves b and c). The amperometric current owing to the oxidation of H_2O_2 with the same concentration obtained from the NPTs/CFMDE is approximately 20 times of that from the Pt/CFMDE, while the background current and noise do not show an obvious increase. The detection limit ($S/N = 3$) of H_2O_2 on NPTs/CFMDE is 5.0×10^{-9} M, which is, to our knowledge, the lowest among the H_2O_2 microelectrochemical sensor reported. The results show that the Pt nanoparticles homogeneously dispersed by the nanostructures in Nafion afford high specific surface area for electrochemical detection of H_2O_2 . Furthermore the NPT/CFMDE displays a very quick response time (Figure 3B, inset). The linear response is given by the equation $y = 0.6444x + 0.07861$ ($R^2 = 0.9982$) (Figure 3B), where y is the amplitude of the amperometric response in picoamps and x is the H_2O_2 concentration in nanomolar.

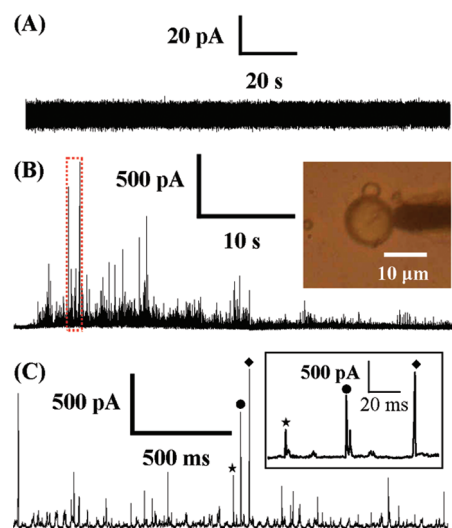


Figure 4. Amperometrically monitoring the oxidative burst on a single protoplast from the leaf of susceptible oilseed rape genotype (215). (A) No current spikes were recorded when the protoplasts were not stimulated by BTH. (B) Amperometric signals showing the large numbers of transient oxidative microburst events from a living protoplast evoked by BTH. The oxidative microburst events inside the broken line frame in part B are amplified in part C, and the three marked events are magnified in the inset.

Immobilization of Plant Protoplasts. The plant cells must be kept in a fixed position during the whole stimulation and monitoring process. While unlike mammalian cells which can be easily adhered to a poly-L-lysine (PLL) precoated substrate, the plant protoplasts could hardly be immobilized by the reagents used to promote the adherence of mammalian cells. In this article, we developed the use of a coating of 0.15% gelatin on the glass substrate, on which the oilseed rape protoplasts were successfully immobilized. Furthermore, the results from fluorescent dyeing showed that most of the protoplasts (>90%) after adherent to gelatin for 7 h and subsequent in PBS for 1 h maintain good viabilities, which facilitate the oxidative burst from single living plant protoplasts to be real-time electrochemically monitored.

Real-Time Monitoring of Oxidative Burst from Single Living Protoplasts. Using the novel NPTs/CFMDEs, we amperometrically investigated the oxidative burst from the protoplasts of oilseed rape, a model plant that have been widely biologically and systematically investigated. Benzothiadiazole (BTH), a synthetic systemic acquired resistance (SAR) inducer was used as the stimulant to induce an oxidative burst from living protoplasts, for the enhancement of ROS generation was thought to be part of the mechanism of BTH-induced SAR.^{40,41}

The amperometric results by single living protoplasts from oilseed rape leaves triggered by BTH are presented in Figures 4 and 5. Obvious amperometric signals were obtained on the protoplasts from both the susceptible (wild type, 215, Figure 4) and glucose oxidase(GOx)-transgenic oilseed rape (high resistance type, GB014, Figure 5). The results showed that the oxidative burst from a single protoplast evoked by BTH led to large numbers of transient amperometric spikes, each spike was

(40) Görlach, J.; Volrath, S.; Knauf-Beiter, G.; Hengy, G.; Beckhove, U.; Kogel, K.; Oostendorp, M.; Staub, T.; Ward, E.; Kessmann, H.; Ryals, J. *Plant Cell* **1996**, *8*, 629–643.

(41) Yang, Y.; Shah, J.; Klessig, D. F. *Genes Dev.* **1997**, *11*, 1621–1639.

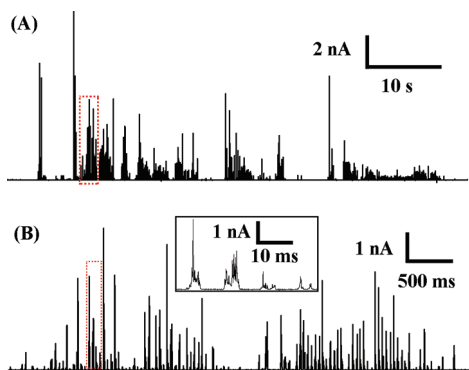


Figure 5. Amperometrically monitoring the oxidative burst on single protoplast from a leaf of glucose oxidase-transgenic oilseed rape genotype (GB014, high resistance type). (A) The oxidative burst from GB014 genotype display a dramatic elevation in ROS concentration. The oxidative microburst events inside the broken line frame in part A are amplified in part B, and the oxidative microburst events inside the broken line frame in part B are amplified in the inset.

Table 1. Mean Values of Quantitative and Kinetic Parameters of Amperometric Spikes from the Oxidative Bursts on Individual Oilseed Rape Protoplasts

oilseed rape genotypes	percentage ^a	I_{\max} [pA]	t_{spikes} [ms]
215 ^b	36.7% ($n = 120$)	141.34 ± 10.56	5.20 ± 0.34
GB 014 ^c	72.7% ($n = 150$)	1020 ± 60	9.87 ± 0.24

^a Percentages of protoplasts from which an oxidative burst can be detected. ^b Susceptible oilseed rape, 235 spikes from 9 protoplasts. ^c Glucose oxidase-transgenic oilseed rape, 368 spikes from 9 protoplasts.

corresponding to a single “oxidative microburst event”. The “transient oxidative microbursts” from the plant protoplast is quite different from the characteristics of the oxidative burst at the single mammalian cells in which case the oxidative burst usually results in a single spike-shaped amperometric signal that can usually last for a few to tens of minutes.^{12–14} Furthermore, the characteristic of oxidative microburst on the single protoplast is also different from the behaviors detected on the oilseed rape leaves (previous measurements showed that an increase of single amperometric signal that lasted for several hours was recorded as a result of the oxidative burst from the infected leaves).⁴² The different oxidative burst characteristics between the single protoplast and the leaf tissue measurements indicated that the mechanisms of ROS production and the oxidative burst could possibly be revealed by real-time monitoring at single cell levels.

Quantitative and Kinetic Characteristics of Oxidative Burst from Single Plant Protoplasts. Some quantitative and kinetic parameters of the oxidative burst from the single protoplasts are summarized in Table 1. The t_{spike} (the width of the baseline of single transient spikes) is used instead of $t_{1/2}$, since most of the spikes displayed complex features (Figure 4C and Figure 5B). Under the stimulation of BTH, the ROS release reaches to a high concentration in a short time, which is consistent with previous results that the protective action in plant cells under stress conditions was usually overridden by the oxidative burst-

rapid and transient production of high levels of H_2O_2 .^{43,44} The average t_{spike} are 5.20 ± 0.34 and 9.87 ± 0.24 ms for the single oxidative microburst events from 215 and GB 014 genotypes, respectively, which shows that the single oxidative microbursts occur at a very short time scale. Furthermore, the large numbers of transient current spikes indicated that the oxidative burst from a single plant protoplast is possibly via a “quantum” kinetic characteristic, which is similar to the behaviors of neurotransmitters or hormones secreted from neurons and neuroendocrine cells by exocytosis.

Compared with the 215 genotype protoplasts, the oxidative burst evoked by BTH protoplasts from GB014 genotype showed a distinguished elevation in ROS production (1.02 ± 0.06 nA vs 141.34 ± 10.56 pA) and longer-lasting (14–15 min vs 6–7 min). Biological results demonstrated that the plants expressing the glucose oxidase (GOx) gene displayed much better disease-resistance, owing to the possible mechanism of the enhancement of H_2O_2 generation by the specific enzyme-catalyzed oxidation of glucose. In our experiments, this possible mechanism is evidenced by direct monitoring at the single plant cell level.

DISCUSSION

H_2O_2 is a vital messenger molecule, which can act as a local signal for hypersensitive cell death (hypersensitive response, HR) to prevent the diffusion of infection and also as a diffusible signal for the induction of defensive genes in adjacent cells (SAR). In response to pathogen attack or infection, the elevation of salicylic acid (SA) in the plant leads to suppression of endogenous peroxidase activity as a result of the binding between SA and SA binding protein (SABP, a peroxidase homologue), which finally resulted in the oxidative burst characterized by elevation of the production H_2O_2 and oxygen radicals. BTH, a synthetic chemical potent inducer of both resistance and gene induction, has much higher binding affinity to SABP than SA and has been developed as an efficient plant protection compound that works by inducing the plant’s inherent disease resistance mechanisms.^{40,41} Furthermore, plants expressing a gene encoding glucose oxidase (GOx) exhibited enhanced resistance because of the elevated levels of H_2O_2 production owing to the oxidation of glucose catalyzed by GOx.

The BTH induced oxidative burst from plants and the enhanced ROS production from transgenic plants have been investigated on plant tissues; however, the oxidative burst from single plant cells has not been well demonstrated. Here, we electrochemically monitored in real-time the oxidative burst from single plant cells using novel microelectrochemical sensors we developed in this article. The BTH induced SAR by a rapid burst of ROS production, and the elevated levels of ROS from transgenic plant have been directed monitored at the single cell level for the first time. The best proof of the biological relevance of the results presented here is given by their agreement with those obtained by traditional biological assay. Moreover, the kinetic and quantitative characteristics of microburst events from single protoplasts have also been demonstrated.

(43) Jacks, T. J.; Davidonis, G. H. *Mol. Cell. Biochem.* **1996**, *158*, 77–79.

(44) Bolwell, G. P.; Wojtaszek, P. *Physiol. Mol. Plant Pathol.* **1997**, *51*, 347–366.

CONCLUSIONS

In this study, we have fabricated a novel NPs/CFMDE by depositing Pt nanoparticles on the nanopores containing polymer matrix coated CFMDEs, and this technique would provide new ideas for the development of sensitive microelectrochemical sensors. Furthermore, we amperometrically monitored in real-time the oxidative burst from individual living plant protoplasts for the first time. The “quanta microburst” characteristics were well demonstrated, and the protoplasts from the transgenic plants biologically that displayed better disease-resistance show a distinguished elevation and longer-term lasting oxidative burst. However, the results presented here are still insufficient for revealing the oxidative mechanism in the plant, and it would facilitate a better understanding of the roles that oxidative burst plays in plant disease defense and signal transduction.

ACKNOWLEDGMENT

This work was supported by the National Natural Science Foundation of China (Grant Numbers 20675060 and 90717101) and the Science Fund for Creative Research Groups (Grant No. 20621502), National Basic Research Program of China (973 Program, Grant No. 2007CB714507) and the Fund for Distinguished Young Scholar of Hubei Province (Grant No.2007ABB023), and the Chenguang Project for Youth of Wuhan City (Grant No. 200850731368).

Received for review June 16, 2009. Accepted August 31, 2009.

AC901300B